



The Japan Society for Precision Engineering

Introduction of JSPE Best Paper Awards 2017

1. An optical lever by using a mode-locked laser for angle measurement

Yuki SHIMIZU, Yukitoshi KUDO,
Yuan-Liu CHEN, So ITO and Wei GAO
Precision Engineering, Vol.47, pp.72-80

A new concept of optical lever for angle measurement having an extended angular measurement range with a mode-locked laser as the light source, which is significantly extended from the conventional photodiode (PD)-type optical levers with a single frequency laser, is proposed. In the proposed concept, a collimated laser beam of the mode-locked laser is made incident to a grating reflector to generate a group of first-order diffracted beams from the grating reflector. Differing from a conventional PD-type optical lever employing a laser beam with a single frequency as the light source, the angle measurement range can be significantly expanded for the sake of the group of widely-spread first-order diffracted beams. In addition, the proposed optical lever has a potential of assuring the traceability of angle measurement by linking it to the optical frequency comb based on the mode-locked laser, which is employed as the national standard of time and frequency. In this paper, as a first step of this research, a mode-locked femtosecond laser is employed as the light source of the proposed optical lever. To distinguish each of the first-order diffracted beams generated with the combination of the mode-locked femtosecond laser and the diffraction grating having a grating period of $1.67 \mu\text{m}$, a Fabry-Pérot etalon is employed in the setup of the optical lever to modulate the distance between two neighboring beams in the group of first-order diffracted beams. Experimental setups are developed, and basic experiments are carried out to verify the feasibility of the proposed optical lever.

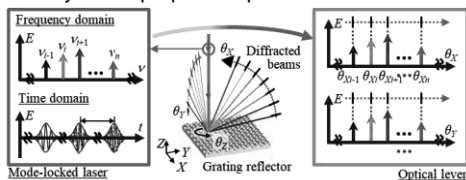


Fig.1 A schematic of the optical lever with a mode-locked laser proposed in this paper

2. Development and precise positioning control of a thin and compact linear switched reluctance motor

Mohd Nazmin MASLAN, Hikaru KOKUMAI
and Kaiji SATO

Precision Engineering, Vol.48, pp.265-278
This paper describes the development and precise positioning control of a thin and compact linear switched reluctance motor (LSRM). The LSRM that has been developed has a mover that is easy to fabricate and can be

disposable. The mover can be easily separated from the stator, allowing it to be changed frequently or discarded in a hazardous application. The prototyped LSRM mover is only 0.128 mm thick with the stator measuring 2.0 mm at its thickest point. These features are highly desirable for space savings while being cost-effective. However, the LSRM has a strong nonlinear driving characteristic that presents a challenge with respect to precision control. In order to overcome this problem and achieve precision positioning, a linearizer unit was designed and integrated into the controller to compensate for the nonlinear relationships among the effective thrust force, mover position, and excitation current. The usefulness of the designed controller was examined experimentally. The experimental positioning results show that the steady-state errors were all less than $1 \mu\text{m}$ in the working range of the LSRM. In addition, the redesign for the improvement of thrust characteristic and easy fabrication of the LSRM is explained.

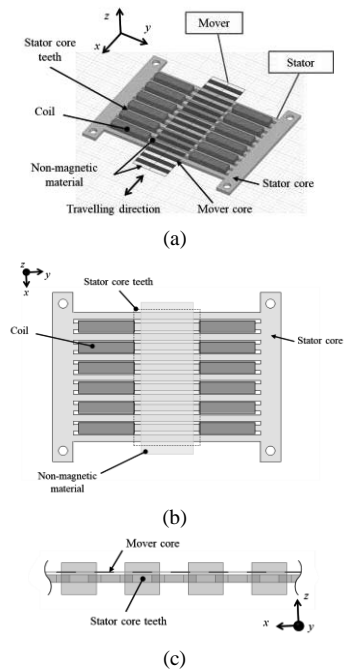


Fig.2 Basic structure of the LSRM (a) 3-D view (b) Top view of stator (c) Cross-sectional view

3. Influence of rotary axis on tool-workpiece loop compliance for five-axis machine tools

Daisuke KONO, Yuki MORIYA
and Atsushi MATSUBARA
Precision Engineering, Vol.49, pp.278-286

This study investigated the influence of the rotary axis of a 5-axis machine tool on the tool-workpiece compliance. The evaluation focused on the influence of the rotation angle and clamping condition of the B axis on the compliance variation. A method was determined to calculate the tool-workpiece compliance in an arbitrary direction from compliances

measured using orthogonal triaxial excitations. Then, the tool-workpiece compliance of a 5-axis machine tool was evaluated and displayed using a color map. The compliance map showed that the magnitude of the compliance varied by up to 40% with changes in the B axis rotation angle and its clamping condition. A drastic change in the negative real part of the compliance was also detected in the compliance map. The results of an experimental modal analysis are used to discuss the cause of the compliance variation. The bending mode of the B axis is an important mode because the change in the bending direction due to B axis rotation has a great influence on the direction dependency of the compliance magnitude and the stability limit. A cutting experiment was conducted to verify the correspondence between the evaluated compliance and the vibrational amplitude in a real cutting process. The compliance variation in the compliance map corresponded to the amplitude variation of the vibration in an end milling process. The compliance map revealed that the vibration synchronized with the passing cycle of cutters was decreased by 80% by unclamping the B axis.

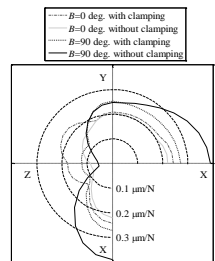


Fig.3 Comparison of the maximum value of the compliance magnitude

Introduction of JSPE Numata Memorial Paper Awards 2017

1. Deep Metric Learning for Video-Based Person Re-Identification

Naoki KATO, Kohei HAKOZAKI,
Masamoto TANABIKI, Yuji SATO,
Junko FURUYAMA and Yoshimitsu AOKI
J. JSPE, Vol.83, No.12, pp.1117-1124

This paper proposes a novel approach for video-based person re-identification that exploits deep convolutional neural networks to learn the similarity of persons observed from video camera. By Convolutional Neural Networks (CNN), each video sequence of a person is mapped to a Euclidean space where distances between feature embeddings directly correspond to measures of person similarity. By improved parameter learning method called Entire Triplet Loss, all possible triplets in the mini-batch are taken into account to update network parameters at once. This simple change of parameter updating method significantly improves network training, enabling the embeddings to be further discriminative. Experimental results show that proposed model achieves new state of the art identification rate on iLIDS-VID dataset and PRID-2011 dataset with 78.3%, 83.9% at rank 1, respectively.

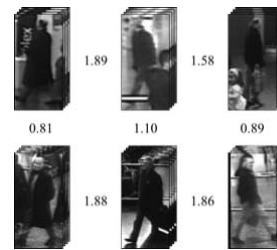


Fig.4 Output distances of our network between each pair of sequence. Vertically aligned pairs are the same person and horizontally aligned pairs are different persons. Larger distance value indicate that the pair is dissimilar. A threshold of 1.3 classifies all the pairs properly

2. Design of ECM tool electrode with controlled conductive area ratio for holes with complex internal features

Dahai MI and Wataru NATSU

Precision Engineering, Vol.47, pp.54-61

The design method of electrochemical machining (ECM) tool electrode with controlled conductive area for the machining of holes with given complex internal features was presented in this paper. Such holes were difficult to machine with traditional mechanical machining methods. In authors' previous work, it has been proved that electrochemical machining (ECM) using tool electrode with controlled conductive area ratio was effective to machine many kinds of complex holes. However, it is considered that the inverse problem, i.e., designing of suitable tool electrode for given internal feature is of great importance for practical application. Therefore, in this work, the proposed ECM process was modeled to investigate the electric potential and current distribution in the electrolyte and on the electrodes' surface, and the evolution of inner hole profile. Then, the relationship between conductive area ratio and the machining depth was investigated by a set of fundamental simulation experiments. Simulation result showed that suitable tool electrode with specific helical conductive area can be designed for the machining of hole with given internal feature. A prototype tool electrode with non-uniform conductive area ratio from its tip to the root was fabricated and used in the verification experiment. The machining result showed that a free-formed hole was successfully shaped and the inner hole profile is in well accordance with the given internal feature.

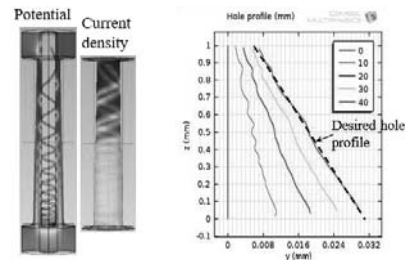


Fig.5 Simulation results with designed electrode (a) Potential and current density distribution at Time=40s, (b) Hole profile at Time=0s, 10s, 20s, 30s and 40s